

Figure S1

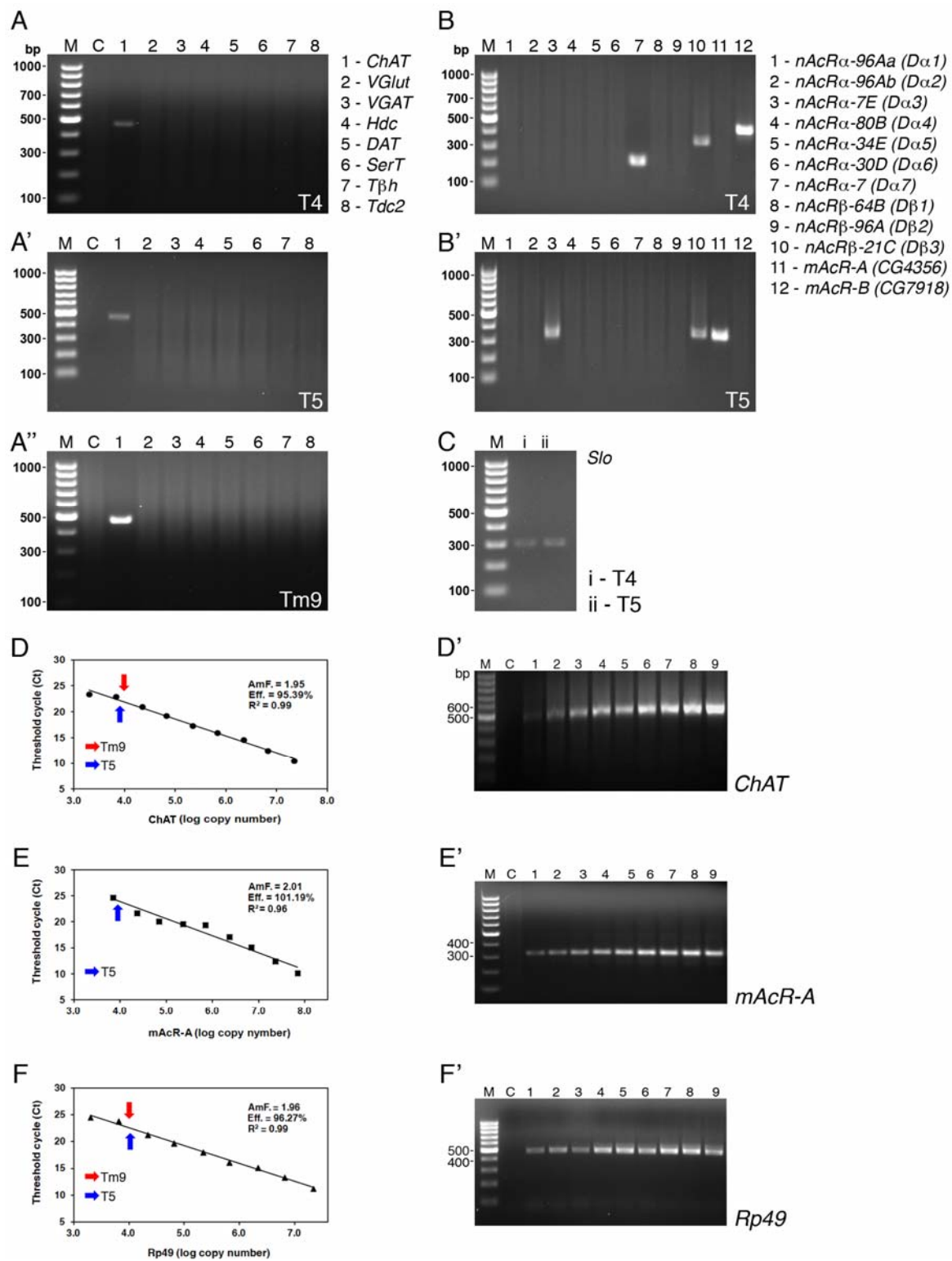


Figure S1: Transcript profiles of T4, T5 and Tm9 neurons reveal their expression of transcripts for neurotransmitter transporters and biosynthesis enzymes, as well as cholinergic receptors and the potassium channel Slowpoke.

(A) T4 cells. (A') T5 cells. (A'') Tm9 cells. PCR-amplified products of the transcripts from single Gal4-driven GFP-expressing neurons. Choline acetyl transferase (*ChAT*) transcript appears in T4, T5 and Tm9. Lane M: 100bp DNA ladder marker; lane C: negative control (without reverse transcription). 1: *ChAT*; 2: *VGlut*; 3: *VGAT*; 4: *Hdc*; 5: *DAT*; 6: *SerT*; 7: *Tβh*; and 8: *Tdc2*

(B, B') PCR-amplified products of cholinergic receptor transcripts from single T4 (B) and T5 (B') cells. T4 neurons express two nicotinic receptor subunits, *Dα7* and *Dβ3*, as well as the muscarinic receptor *mAcR-B* (CG7918). T5 neurons express two nicotinic receptor subunits, *Dα3* and *Dβ3*, as well as a different muscarinic receptor, *mAcR-A* (CG4356). Lane M: 100bp DNA ladder marker; 1: *nAcRα-96Aα* (*Dα1*); 2: *nAcRα-96Ab* (*Dα2*); 3: *nAcRα-7E* (*Dα3*); 4: *nAcRα-80B* (*Dα4*); 5: *nAcRa-34E* (*Dα5*); 6: *nAcRa-30D* (*Dα6*); 7: *nAcRα-7* (*Dα7*); 8: *nAcRβ-64B* (*Dβ1*); 9: *nAcRβ-96A* (*Dβ2*); 10: *nAcRβ-21C* (*Dβ3*); 11: *mAcR-A* (CG4356); 12: *mAcR-B* (CG7918).

(C) PCR-amplified products of the potassium channel *slowpoke* transcripts from T4 (lane i) and T5 (lane ii). Lane M: 100bp DNA ladder marker.

(D-F) Standard curves for T5 cells generated by plotting *CT* values against the known initial DNA copy number. Abscissa is the logarithm of the input cDNA; ordinate is the number of PCR cycles required to reach a given fluorescence signal level (*Ct*). Threshold cycle, *CT*, values (ordinate) were obtained using a controlled amount of input cDNA for *ChAT* (D); *mAcR-A* (E); and *Rp49* (F). The final PCR product was analyzed by DNA gel electrophoresis (D', E', F'). *Ct* and the logarithm of the input cDNA varied in inverse linear proportion over a large concentration range. Standard linear regression analysis was used to calculate the standard curve, the amplification factor (AmF), PCR efficiency (Eff), and the coefficient of determination (R^2) for each curve. The standard curves were used to calculate the *ChAT* [D] and *mAcR-A* transcript level in Tm9 (red arrows) and T5 (blue arrows) neurons. All qRT-PCR amplification reactions were carried out in three biological replicates for each cell type.

(D') Lane M: 100bp DNA ladder marker; lane C: negative control (without reverse transcription). Lanes 1-9: *ChAT* amplicon using different amounts of input DNA (D). (E') as in (D') but for *mAcR-A*. (F') as in (D') but for *Rp49*.

Table S1: The numbers of input synapses from four classes of Tm cell input (Tm1, Tm2, Tm9, Tm4) to their T5 target cells

	Tm1	Tm2	Tm9	Tm4	other or unknown	total
T5-01	7	14	8	3	3	35
	20.00	40.00	22.86	8.57	8.57	100
T5-02	6	12	11	6	3	38
	15.79	31.58	28.95	15.79	7.89	100
T5-08	8	12	10	3	3	36
	22.22	33.33	27.78	8.33	8.33	100
T5-11	7	11	9	5	3	35
	20.00	31.43	25.71	14.29	8.57	100

	Tm1	Tm2	Tm9	Tm4	other or unknown	total
T5-03	7	8	10	4	5	34
	20.59	23.53	29.41	11.76	14.71	100
T5-04	6	18	1	4	5	34
	17.65	52.94	2.94	11.76	14.71	100
T5-15	9	8	6	8	4	35
	25.71	22.86	17.14	22.86	11.43	100
T5-16	7	9	9	5	6	36
	19.44	25.00	25.00	13.89	16.67	100

For each combination of a particular T5 cell and input terminal, the upper number indicates the number of synaptic contacts observed and the lower number the percentage these constitute of all synaptic inputs to that T5 cell.

Table S2: Fly stocks used in this study.

For immunolabeling T4, T5, Tm9 and Tm1 neurons, flies with the following genotypes were used:

- (1) For T4: *yw/w; UAS-mCD8GFP/+; R54A03-GAL4/UAS-mCD8GFP* (Maisak et al., 2013).
- (2) For T5: *yw/w; UAS-mCD8GFP/+; R42H07-GAL4/UAS-mCD8GFP* (Maisak et al., 2013).
- (3) For Tm9: *yw/w; UAS-mCD8GFP/+; vGlu⁶⁷⁸⁰-Gal4/+* (Ting et al., 2014).
- (4) For Tm1: *yw/w; ; 27b-Gal4/UAS-mCD8GFP* (Morante and Desplan, 2008).

For single-cell transcript profiling experiments, flies with the following genotypes were used.

- (1) For T4: *w; UAS-mCD8GFP/UAS-mCD8GFP; VT37588-GAL4/UAS-mCD8GFP*
or *w; UAS-mCD8GFP/UAS-mCD8GFP; R54A03-GAL4/UAS-mCD8GFP* (Maisak et al., 2013).
- (2) For T5: *w; UAS-mCD8GFP/UAS-mCD8GFP; R42H07-GAL4/UAS-mCD8GFP* (Maisak et al., 2013).
- (3) For Tm9: *yw/w; UAS-mCD8GFP/+; vGlu⁶⁷⁸⁰-Gal4/+* (Ting et al., 2014).

Supplemental Experimental Procedures

Procedures to locate synaptic inputs and their distributions over T5 arbors

Raw ~1800 x 1300 pixel EM images were stitched together using software PTGui (New House Internet Services B. V., The Netherlands) to cover an area about 35 μm x 45 μm , roughly 8000 x 6000 pixels. The stitched images were subsequently imported to Fiji software as an image stack (Schindelin et al., 2012). To align the images, we used a Fiji plug-in StackReg (Thévenaz et al., 1998). After alignment, the images were imported as a stack to TrakEM2, another Fiji plug-in, for tracing and further analyses.

Dendritic arbors of T5 cells with targeted membrane HRP expression were traced by painting their profile areas. After the dendrites of a particular T5 cell were fully traced, presynaptic sites of Tm cell terminals that provided inputs were identified. Active zones of the presynaptic terminals are characterized by electron-dense T-bar ribbons, appearing as darker T-shaped profiles approximating the cytoplasmic side of the plasma membrane. Each was usually accompanied by many synaptic vesicles and located adjacent to the tips of T5 dendrites, which typically had a diameter <100nm, much thinner than T5's axonal neurites. Presynaptic terminals were traced back from their synaptic sites to encompass the entire terminal and thereby reveal its identity. Occasional terminals lacking a clear morphological identity were designated "unidentified". Postsynaptic sites were plotted over the surface of reconstructed T5 cell arbors (Figures 3A-L). Spatial coordinates for each synaptic site were determined, and the averaged coordinates and standard deviations calculated for the grouped pairs of input and output neurons (Figure 3N).

Supplemental References

- Schindelin, J., Arganda-Carreras, I., Frise, E., Kaynig, V., Longair, M., Pietzsch, T., Preibisch, S., Rueden, C., Saalfeld, S., Schmid, B., Tinevez, J.Y., White, D.J., Hartenstein, V., Eliceiri, K., Tomancak, P., and Cardona, A. (2012). Fiji: an open-source platform for biological-image analysis. *Nature Methods* 9, 676-682.
- Thévenaz, P., Ruttimann, U. E., and Unser, M. (1998). A pyramid approach to subpixel registration based on intensity. *IEEE Transactions on Image Processing* 7, 27-41.